MUHAMMAD BURHAN KHAN[1, 2], HUMAIRA NISAR[3], CHOON AUN NG[4]

GENERALIZED MODELING OF THE SLUDGE VOLUME INDEX AND SUSPENDED SOLIDS TO MONITOR ACTIVATED SLUDGE BIOFLOCCULATION USING IMAGE ANALYSIS

The performance of an activated sludge wastewater treatment plant depends on bioflocculation that is monitored by physical measurements such as the sludge volume index (SVI) and mixed liquor suspended solids (MLSS). The estimation of SVI and MLSS has been proposed using image analysis based modeling which is time-efficient and valid for multiple plants operating in different states. The methodology includes the sequence of image acquisition using bright-field microscopy, a robust segmentation of flocs, partitioning of flocs based on different ranges of their equivalent diameters, extraction of morphological features, and modeling of SVI and MLSS using the features. It is proposed that bright-field microscopy at lower magnification to capture the flocs is sufficient to model SVI and MLSS. A robust approach for image segmentation is adopted by integrating state-of-the-art image segmentation algorithms. It is hypothesized that flocs in different ranges of equivalent diameter respond differently to the variation in the operating state. Hence, flocs and their respective image analysis features are categorized based on the range of equivalent diameter. Finally, stepwise regression is used for feature selection and model identification to explore the feasibility of generalization of models to multiple plants in different states regarding SVI and MLSS.

1. INTRODUCTION

The activated sludge process is widely used to treat municipal and industrial influent flowing into the wastewater treatment plants. The quality of the effluent depends on bioflocculation, settling properties of flocs, and the presence of filamentous bacteria. Flocs are microbial aggregates and comprise dead and alive microorganisms and their metabolism products. Filamentous bacteria are found as protruding or free filaments and

_____

[1]Department of Electronic Engineering, Universiti Tunku Abdul Rahman, Kampar 31900, Malaysia.

[2]Department of Electrical Engineering, National University of Computer and Emerging Sciences, Karachi, Pakistan.

[3]Department of Electronic Engineering, Universiti Tunku Abdul Rahman, Kampar 31900, Malaysia, corresponding author, e-mail address: humaira@utar.edu.my

[4]Department of Environmental Engineering, Universiti Tunku Abdul Rahman, Kampar 31900, Malaysia.

form the backbone of the flocs. They may affect the settling of the flocs if they are present in very large or very small number [1]. The solid-liquid separation problem in the clarifier arises if flocs do not settle due to abnormal operating state of the activated sludge process such as of pin-floc, dispersed growth and bulking. The process is conventionally monitored by physical measurements such as the sludge volume index (SVI) and mixed liquor suspended solids (MLSS) [2]. The measurement of SVI and MLSS is time-consuming and involves environmental and economic costs. Image processing and analysis is a cost-effective and time-efficient alternative to conventional measurements. For example, MLSS requires regulated heating for at least an hour. Image acquisition, processing, analysis, and subsequent estimation take 15–20 minutes (depending on the population of the flocs) to estimate MLSS of a sample for a plant [3, 4].

To use image processing and analysis concerning the activated sludge process, microscopic images are acquired by using samples collected from aeration tanks of the activated sludge wastewater treatment plant. The acquired images are segmented for flocs and filamentous bacteria. In this paper, image analysis data of flocs has only been used, thereby showing that the segmentation of flocs is sufficient to estimate SVI and MLSS.

Accuracy of image segmentation is a fundamental requirement for accurate and precise image analysis. Several authors have reported the segmentation of bright-field microscopic images of activated sludge samples. The basic image processing approaches of Canny's algorithms [5], histogram-based inter-means algorithm [6], and image enhancement with edge detection [7] have been reported in the literature. Perez et al. [8] proposed a sequence of background correction, histogram equalization, median filtering, and morphological analysis for the bright-field activated sludge images. The aforementioned algorithms did not address the artifacts associated with the microscopy and were reported without their objective assessment. The bright-field microscopy has only been used due to its simple procedures of sample preparation and image acquisition.

Bright-field activated sludge images have the problem of irregular illumination in addition to the weak contrast between the flocs and the background. Therefore, global thresholding techniques usually do not perform well due to irregular illumination, also termed as vignetting [9]. The individual algorithms segment some activated sludge images accurately but fail for other images due to randomness in the population, size, and non-smooth boundaries of flocs. In this paper, an integrated segmentation approach is used, employing variations of one or multiple state-of-the-art algorithms such as mean-C local thresholding [10], and local adaptive Otsu [11]. As far as the image analysis of activated sludge images is concerned, different image analysis features have been reported in the literature [12]. Generally, those features are reported regarding correlation with the measurements such as SVI and MLSS. Amaral et al. [13] suggested the identification of four states of an experimental setup of activated sludge plants with synthetic feed, using image analysis features and epifluorescence microscopy. They suggested the possibility of measurement of SVI and MLSS by showing a correlation between image analysis features and the physicochemical data. They also used partial least square

(PLS) analysis to estimate SVI and MLSS [13]. The approach reported in this paper is different because bright-field microscopy and image analysis of flocs only have been employed without requiring any staining procedures.

In another approach, neural networks were used to estimate SVI. For the neural networks, either physicochemical and/or image analysis features were used as input. Boztoprak et al. [14] suggested the use of a neural network to predict SVI. Thirty-three image analysis features of flocs and filaments were used as input to the neural network. Tomperi et al. [15] modeled the suspended solids using incoming iron concentration, mean and median area of flocs, and amount of filaments. Very recently, real-time optical monitoring of the wastewater treatment plant was proposed by the image analysis-based optimal models [16]. Honggui et al. [17] proposed a fuzzy neural network-based modeling of SVI using physicochemical measurements as input to the network. The measurements included total nutrients, chemical oxygen demand, pH, and dissolved oxygen. In this paper, image analysis data of flocs has been used to estimate SVI and MLSS. The state of the wastewater treatment plants has been tracked by estimating important physical parameters of the plant using image analysis based modeling.
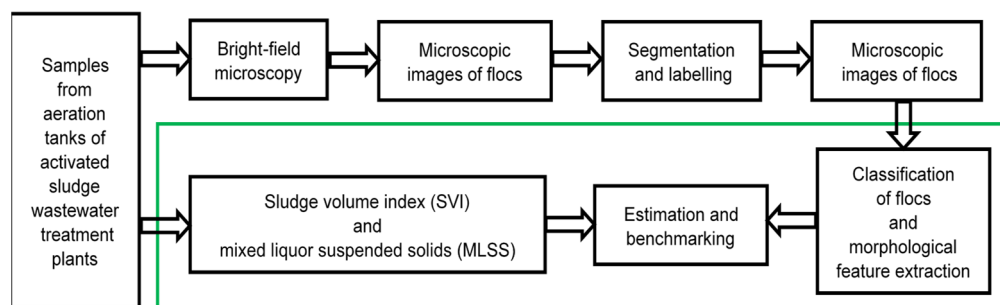

Fig. 1. Workflow for the estimation and its generalization to multiple plants using bright-field microscopy

In this research, it is proposed to estimate SVI and MLSS using image analysis of flocs and regression models, as an alternative to the physical methods. The proposed strategy is distinct in the sense that the flocs are considered at 4x objective magnification using only bright-field microscopy with simple image acquisition protocol. The proposed protocol and procedures require less time to acquire images of the entire sample and estimate SVI and MLSS. A shared data scenario is also investigated for the possibility of generalization of the regression models to other activated sludge plants. The image analysis features were also explored for their usefulness to predict SVI and MLSS, for different ranges of equivalent diameter. The workflow of this work is shown in Fig. 1. This work may be viewed as an extension of our previous work [4], however, it is significantly distinct in the following ways. First, more samples from eight municipal activated sludge wastewater treatment plants are included in this study in addition to the samples from an experimental setup. Second, the modeling of MLSS has been

suggested, besides a more elaborate assessment of the significance of the floc classification for both SVI and MLSS. Third, the generalization of the models has been explored in the sense of their applicability to multiple activated sludge wastewater treatment plants operating in different states.

2. METHODS

2.1. EXPERIMENTAL SETUP AND DATA ACQUISITION

Experimental setup of activated sludge wastewater treatment plant was fabricated with an aeration tank of size 5.4 dm^3. The setup was inoculated with activated sludge collected from aeration tank of a municipal wastewater treatment plant. The feed of the setup was regularly collected from the influent of the same municipal scale plant to mimic the real process. The hydraulic retention time (HRT) for the plant was varied as 5.4, 10 and 20 days. Previously, it was suggested that nitrogen and phosphorous removal could be enhanced by increasing HRT to 9.3 or beyond 15 days [18]. Therefore, high values of HRT were used to ensure the plant in the normal state with better removal efficiencies. The samples from the aeration tank of the experimental setup and plant K0 were collected weekly. The plant K0 was easily accessible, therefore, more samples could be collected from the plant. The experimental setup was inoculated with the sludge from the same plant. Additionally, samples were also taken from seven more municipal scale wastewater treatment plants monthly. The state of the experimental setup remained normal with SVI above 50 cm^3/g and DO above 7 mg O$_2$/dm^3. The filamentous bacteria were rarely observed in the normal state.

Initially, twenty-six samples from the experimental setup were used to model SVI and MLSS. Later, more samples collected from the municipal wastewater treatment plants were included to investigate if the regression model identified for one plant can be validated by samples from other plants. The details of the number of samples collected from different plants are given in Table 1. The plants have been designated by fictitious codes as required by the operator company. Table 2 shows the number of samples and microscopic images regarding the states of the AS process in the experimental and municipal plants. The following three states have been considered: pin-floc/dispersed growth, normal and bulking. The samples with SVI less than 50 cm^3/g were considered in the pin-floc/dispersed growth. Whereas if SVI is greater than 150 cm^3/g, the state is bulking. The rest of the samples were categorized as a normal state [1].

For image acquisition, 12 mm^3 activated sludge sample was placed on a slide using Biohit Proline Pipette and covered with a cover-slip of size 18 mm×18 mm. The samples were collected from the aeration tanks of the activated sludge wastewater treatment plants, and observed under Olympus microscope BX43 at 4× objective magnification using bright-field microscopy. Low magnification was used for two reasons: first, the filamentous bacteria are not visible at this magnification in the bright-field images, and

second, a smaller number of images are required to cover the entire coverslip. The images were acquired using Olympus CCD camera DP26 interfaced to Intel® Core™ i7-4770 CPU with 8GB RAM running image acquisition software Olympus CellSens Dimension 1.14.

Table 1

Number of samples collected from different
activated sludge wastewater treatment plants

Sample No.	Plants	Number of samples
1	experimental plant	41
2	K1	13
3	K2	4
4	K3	13
5	K4	8
6	K5	5
7	K6	6
8	K7	11
9	K0	29
Total samples		130

As far as the number of images per sample is concerned, on the average, eighty-five images were taken to cover all the floc. The entire coverslip was scanned to acquire the images, along the vertical paths as shown in Fig. 2.
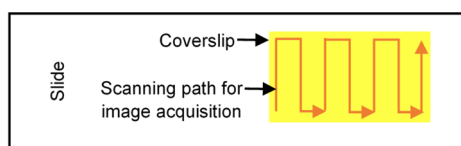

Fig. 2. Scanning path for image acquisition
of bright-field microscopic images of activated sludge

Table 2

States and the respective number of samples and images
collected from plants given in Table 1

State of AS plant	Number of samples	Total number of images
Dispersed growth or pin-floc	54	3782
Normal state	63	5970
Bulking	13	1262
Total images		11 014

The number of total images with respective states of the plants is shown in Table 2. In the case of pin-floc/dispersed growth, there are only a few flocs. Therefore, fewer

images per sample were acquired compared to the normal and bulk states. Total of 130 samples from the experimental setup and municipal wastewater treatment plants were processed for this work. Eleven thousand, fourteen bright-field images were processed for the segmentation and morphological analysis of flocs. The size of each image was 1224×960 pixels with the size of the pixel 1.718 µm/pixel. The algorithms used in this research were implemented on Matlab R2015A.

2.2. IMAGE SEGMENTATION

Image segmentation deals with the partitioning of an image into different regions corresponding to different objects. The problem with state-of-the-art segmentation algorithm was that an algorithm, which worked well for an image, might fail for another image. To minimize any chance of failed segmentation for any of the 11014 images, a segmentation algorithm was devised by integrating several techniques or their variants to segment the flocs in the bright-field microscopic images of AS [3]. The integrated approach towards segmentation was motivated by the incorrect detection of flocs as background. However, the floc pixels are never incorrectly detected as the background. Therefore, some segmentation results from different algorithms are scanned in the integrated segmentation algorithm and identify a pixel as background if it is classified as background by at least one of the segmentations. The following techniques were used for segmentation: illumination compensated global segmentation [19], mean-C local thresholding [10] and local adaptive Otsu [10]. The integration of multiple algorithms adds robustness by leading to successful segmentation even if some state-of-the-art algorithm fails for an image. If background pixels are assigned logical 1 and floc pixels logical 0, logical OR function can be used to integrate the algorithms.

2.3. IMAGE ANALYSIS

The ability of flocs to settle in the clarifier is a major factor to quantify of the performance of the activated sludge process. The flocs appear as flake like objects in the microscopic images with varying morphology and opaqueness. By intuition, the ability of the flocs to settle can be correlated with their morphological features. An ideal floc is the one which has the better settleability and, therefore, is expected to be highly dense, compact, round and non-porous. However, flocs do not have uniform morphological features across a sample. Therefore, the features are calculated for all the flocs and averaged for subsequent estimation of physical parameters. The features of the flocs, considered in this work, are explained in Table 3.

Flocs are grouped as small, medium and large regarding the range of equivalent diameter. However, these ranges were not uniquely defined in the literature [1, 13]. Given different definitions of the groups of flocs and the diverse population of bacteria, it is hypothesized that settling ability of the flocs varies for different ranges of the equiv-

alent diameter, and the morphological features in the ranges. Therefore, the morphological features for each range are calculated and averaged separately. Two different ranges are defined based on the equivalent diameter for small, medium and large flocs [1, 13]. All the range definitions reported in the literature have been included, as shown in Table 4.

Table 3

Morphological features of the flocs and their description

No.	Feature	Description
1	area	total number of pixels in the flocs, scaled by the area of a pixel, μm^2
2	aspect ratio	ratio of major and minor axis length of an ellipse with the same normalized second central moment as that of the floc [20]
3	compactness	$\left(\dfrac{(\pi/4)\ \text{area}}{\text{major axis length}}\right)^{1/2}$ [20]
4	convex perimeter	perimeter of the convex hull
5	convex area	number of pixels contained in the convex region of the floc
6	convexity	ratio of convex perimeter to perimeter [20]
7	eccentricity	ratio of distance between foci of an ellipse with the same second moment as the floc to its major axis length
8	equivalent diameter	diameter of a circle with the same area as that of the floc $((\pi/4\ \text{area})^{1/2})$
9	Euler number	difference between total flocs in the image and holes in those flocs
10	extent	ratio of area of the floc to that of its bounding box.
11	form factor	$\dfrac{4\pi\ \text{area}}{\text{perimeter}^2}$ [20]
12	filled area	area of filled region of floc
13	fractal dimension	an index of variation of complexity with scale measured by box-counting method [21]
14	major axis length	major axis length of an ellipse with the same normalized second central moment as that of the floc
15	minor axis length	minor axis length of an ellipse with the same normalized second central moment as that of the floc
16	perimeter	distance along the boundary of the floc.
17	porosity	$100\left(1-\dfrac{\text{area}}{\text{filled area}}\right)$
18	roundness	$\dfrac{4\ \text{area}}{\pi(\text{major axis length})^2}$ [20]
19	solidity	ratio of area to convex area
20[a]	normalized area	ratio of total floc area to the area captured by all the images

[a]Normalized area is defined for all the flocs in a sample.

Normalized area (N_A) is defined for all the flocs without considering the grouping based on equivalent diameter. Thus, $7 \times 19 + 1 = 134$ features are used. A feature is

denoted by C_x^y, where x indicates the group of the floc as tabulated in Table 4, and y is the feature number as given by the order in Table 3. For example, C_4^4 is a convex perimeter of flocs with an equivalent diameter lower than 150 μm. Previously, a similar approach was proposed concerning floc classification to identify the state of activated sludge wastewater treatment plant [3]. In this work, the classification of flocs has been used from the perspective of the modeling of SVI and MLSS.

T a b l e 4

Floc classification defined by the range of the equivalent diameter

Class of the floc	Equivalent diameter [μm]	Reference
C_0	averaged over all detected flocs	[5, 14, 15]
C_1	<25 (small)	[13]
C_2	25–250 (medium)	
C_3	>250 (large)	
C_4	<150 (small)	[1]
C_5	150–500 (medium)	
C_6	>500 (large)	

2.4. FEATURE SELECTION

Image analysis gave 134 morphological features of the flocs. The next challenge was the selection of the features that could significantly contribute to the modeling of the SVI and MLSS. Stepwise regression was adopted for the feature selection. Stepwise regression adds or removes terms (features or product of features) from a general model based on the p-value of F-statistics. At each step, the p-value is calculated with and without the term, to determine its statistical significance in the prediction of the response. The process of feature selection helped to identify a set of features that should be ignored in the regression. The extended set of features were not found in the literature concerning the range of equivalent diameter of the flocs for feature selection and regression.

2.5. CLASSIFICATION OF FLOCS AND MODELING

One of the main objectives of this work is to identify the equivalent diameter based classes of flocs which can be considered for modeling of SVI and MLSS. It is expected that the classification of the flocs would expectedly decrease the number of features in the process of feature selection, and lead to the construction of better models. The classification from the perspective of the range of equivalent diameter would also give an intuitive explanation of the behaviour of flocs of different sizes under different states of

a plant. Features required for estimation of SVI and MLSS may be different for different plants operating in different states. But the equivalent diameter based classes are expected to be the same for the different plants. It is because the flocs of certain sizes are expected to be more responsive to variations in the state of the plant through variations in their morphological properties. Therefore, the following steps were taken to identify a class or a group of classes of flocs, which may be significant in the modeling of SVI and MLSS.

Stepwise regression is performed for the classes of flocs individually to identify the classes that can contribute to the modeling of the physical parameters (SVI and MLSS). Normalized area (N_A) is also included in the regression along with the features of all the classes of the flocs. Stepwise regression not only does the feature selection but also results in a model [22]. The groups of classes are explored to model the SVI and MLSS using the stepwise regression.

The combinations with the least number of the floc classes and higher adjusted R^2 were identified. Those classes that appeared in the combination were considered to be significant for the estimation of the physical parameters. It was observed if adding a particular class into a group of classes improved the regression model. In this way, starting from individual classes, groups of up to seven classes were investigated using stepwise regression.

Remark. The combination with the least number of classes and higher adjusted R^2 is explained as follows: Consider two classes C_x and C_y, defined based on equivalent diameter. Suppose if C_x and C_y are combined for regression, the adjusted R^2 of $C_x + C_y$ (+ indicates inclusion in regression) gets better than individual adjusted R^2 for both C_x and C_y. If features for another class of flocs, C_z, is included in the doublet $C_x + C_y$, the adjusted R^2 does not get better than individual correlations but is equal to that of $C_x + C_y$. Therefore, $C_x + C_y$ is the combination with the least number of classes and a higher adjusted R^2.

2.6. GENERALIZATION OF ESTIMATION

Finally, it was explored whether generalized models could be found for estimation of physical parameters, which were valid for multiple plants operating in different states. Such universal behavior was suggested to be invalid in the literature [14] because of the complex ecosystem and diversity in the population of bacteria, which were specific to a plant. However, SVI had similar boundaries for the different states of the activated sludge plants [2]. Therefore, it is hypothesized that some universality in image analysis based estimation might also be present. With the recent evolution of e-governance and big data, such a possibility will aid in the centralized monitoring of the wastewater treatment plants. Therefore, a sample has been included from multiple plants in the regression modeling. If the stepwise regression gives poor adjusted R^2, it may be concluded that the same regression model is not feasible for multiple plants. The generalization has been tested for both SVI and MLSS.

3. RESULTS AND DISCUSSION

First of all, the segmentation of the flocs was evaluated subjectively as well as objectively. Subjectively, the segmentations of all the images were found to be appreciably accurate for all the samples from the plants listed in Table 1. The subjective observation was also supported by objective assessment. For objective assessment, gold approximations were prepared for randomly selected forty images. The algorithm achieved an accuracy of 99.38%. Two images randomly selected from the database of the images are shown in Fig. 3, along with their segmentation results.
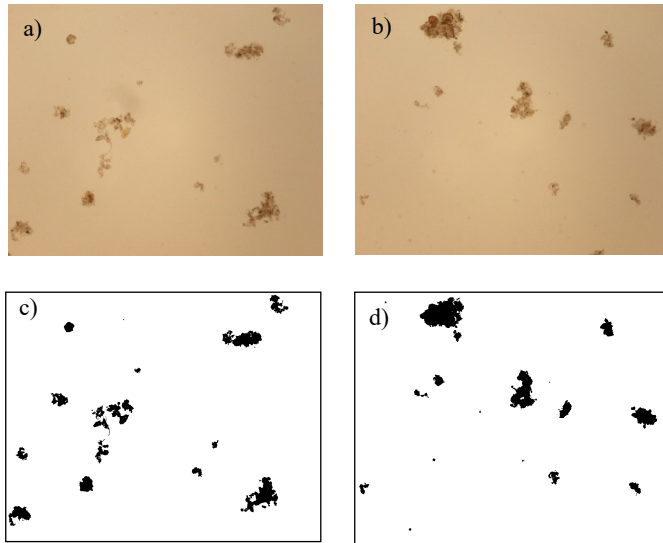

Fig. 3. Bright-field microscopic images of activated sludge samples (a, b),
and their segmentations (c, d)

3.1. VARIATIONS OF IMAGE ANALYSIS FEATURES IN DIFFERENT STATES

To observe the overall variation of physical parameters and image analysis features regarding the state of the plants, the samples are arranged in ascending order concerning SVI. This arrangement gave the first 54 samples of pin-floc/dispersed growth abnormal state, and the last 13 samples of bulking. The samples in between correspond to the normal state as shown by the highlighted areas in Figs. 4–9. The figures show the variations of physical and selected image analysis parameters in the different states. One striking similarity is between MLSS and N_A: both show similar variation in every state as shown in Fig. 5. Similar behavior, though not as explicit as N_A, is shown by perimeter (C_0^{16}) in Fig. 7. In the case of fractal dimension (C_2^{13}), in the state of pin-flocs/dispersed growth, the average trend is increasing as in the case of SVI and MLSS, shown in Fig. 8. However, in a normal

state, the trend of the fractal dimension is decreasing in contrary to the SVI and MLSS. Similar behavior has been shown by the convex area (C_2^5) in Fig. 9.
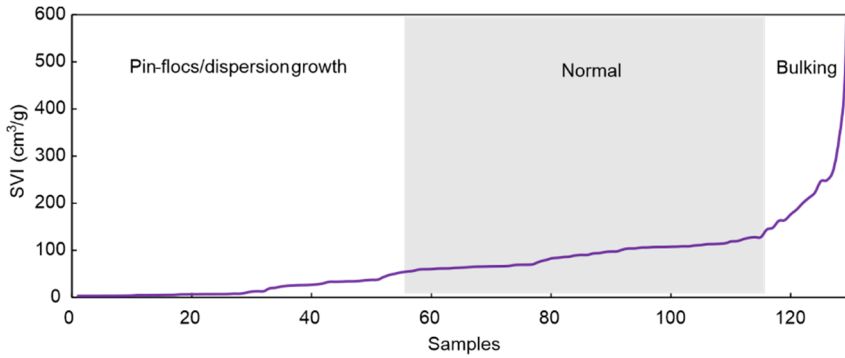

Fig. 4. Variations of sludge volume index (SVI) across the samples
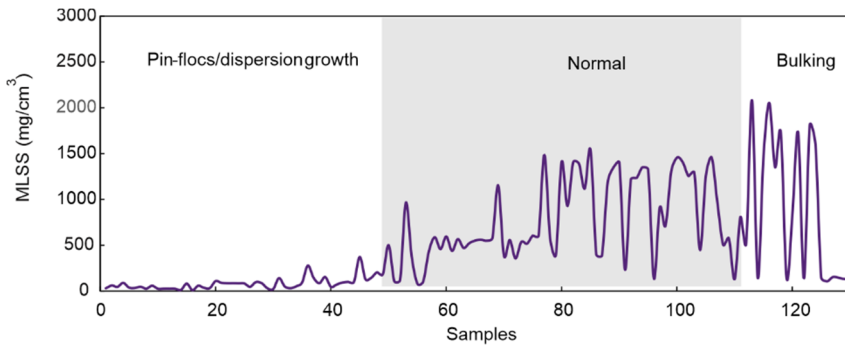referred to the states of the plants

Fig. 5. Variations of mixed liquor suspended solids (MLSS) across the samples
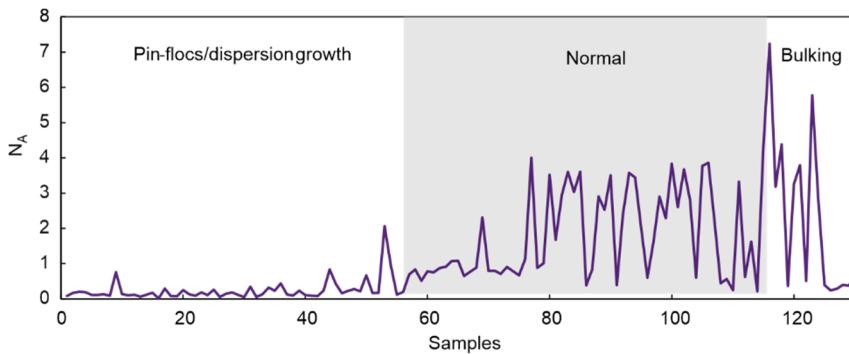referred to the states of the plants

Fig. 6. Variations of normalized area (N_A) across the samples
referred to the states of the plants
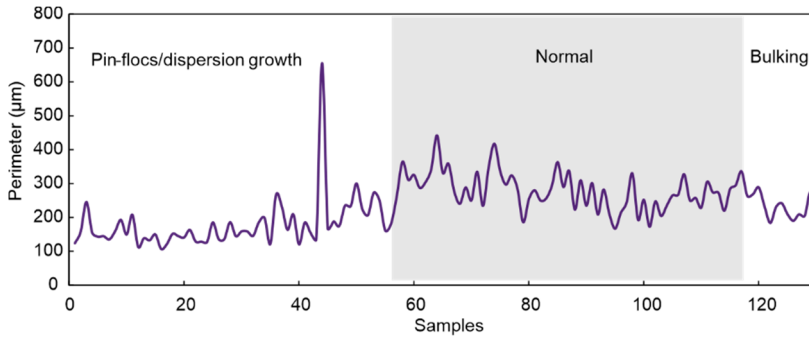
Fig. 7. Variations of C_0^{16} (perimeter) across the samples
referred to the states of the plants
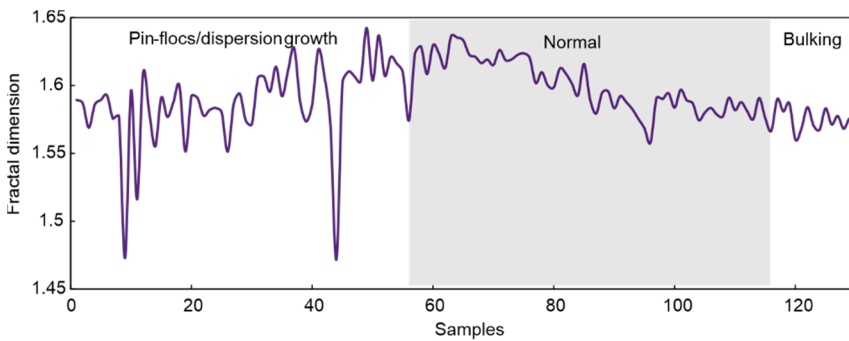
Fig. 8. Variations of C_2^{13} (fractal dimension) across the samples
referred to the states of the plants

Fig. 9. Variations of C_2^5 (convex area) across the samples
referred to the states of the plants

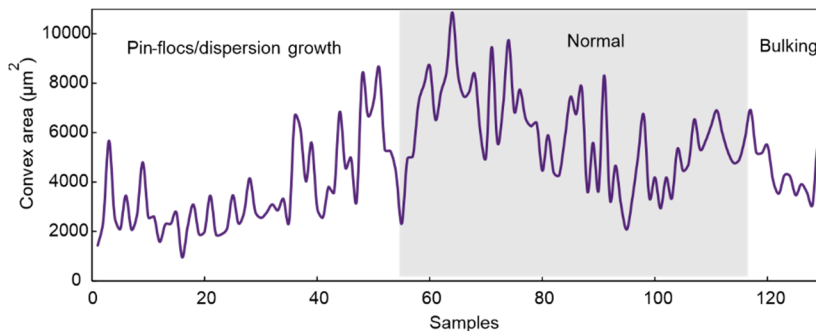In conclusion, it is suggested that some image analysis features show similar trends as the physical parameters irrespective of the state, whereas other features show different variations, depending on the state of the activated sludge plants. Therefore, multiple

parameters are needed to model the AS process, and different variations of parameters in different states may hamper the identification of a model that is valid for multiple plants and their different states.

3.2. ESTIMATION OF SVI AND MLSS WITH FEATURE SELECTION BY STEPWISE REGRESSION

To evaluate the predictability of classes of the flocs, defined in Table 4, the results of Khan et al. [4] were extended to the modeling of MLSS. The SVI modeling has been included again with some improved discussion to make the context and establish the grounds for generalization of the models and the associated significance of the classes of flocs. Thus, twenty-six samples of the experimental setup were used regarding SVI and MLSS separately. The experimental setup was initially in pin-floc/dispersed growth abnormal for the first four samples. The plant was working in the normal state, with SVI between 50 and 150 cm^3/g. Under this state, the filamentous bacteria in the samples are not visible at 4× objective magnification of the microscope using bright-field microscopy. Plants with filamentous bacteria might result in different model and stepwise regression might select a different set of image analysis features. However, the classes of flocs, selected by the stepwise regression, would remain the same. To validate the modeling for other plants, more samples were included from the experimental setup and eight municipal scale activated sludge wastewater treatment plants in the stepwise regression.

Stepwise regression was used for feature selection and regression modeling. This led to the following model where CVI$_{pred}$ is SVI predicted, cm^3/g:

$$SVI_{pred} = 651.51 + 0.07C_3^9 + 0.002C_2^5 - 553.2C_2^{13} + 141.77C_5^2$$
$$+ 409.83C_5^7 - 3.701C_5^{17} - 194.73C_5^2C_5^7 \qquad (1)$$

The selected features concerning the classes of the flocs are tabulated in Table 5, and the regression result is shown in Fig. 10. The model gives an adjusted R^2 of 0.951 with a *p*-value of the order of 10^{-12}.

Table 5

Features selected by stepwise regression for SVI

Class	Features
C_0	–
C_1	–
C_2	convex area, fractal dimension
C_3	Euler number
C_4	–
C_5	aspect ratio, eccentricity, porosity
C_6	–
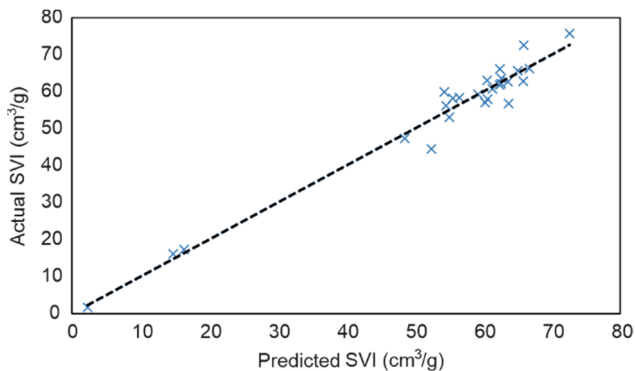
Fig. 10. Estimation of SVI using stepwise regression

Table 6

Features selected by stepwise regression for MLSS

Class	Features
C_0	perimeter
C_1	–
C_2	–
C_3	–
C_4	–
C_5	fractal dimension
C_6	–
–	normalized area
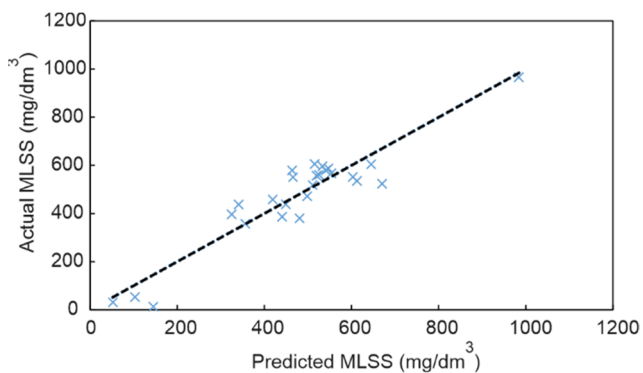
Fig. 11. Estimation of MLSS using stepwise regression

The stepwise regression gave the following model with adjusted R^2 0.884 and p-value of the order of 10^{-10} where $MLSS_{pred}$ is MLSS predicted, mg/dm^3

$$\text{MLSS}_{\text{pred}} = -2818 + 3.656C_0^{16} + 1208C_5^{13} + 1286N_A - 3.426\ C_0^{16}N_A \qquad (2)$$

The resultant features with their respective classes are shown in Table 6. The scatter plot for the model is shown in Fig. 11.

The features selected by stepwise regression for SVI belonged to the classes C_2, C_3, and C_5. Whereas the features for MLSS were from the class C_0 and C_5 with an additional feature of N_A. The N_A individually has a correlation of 0.835 with MLSS, and 0.49 with SVI. The result shows the distinctive role of the classes of the flocs and respective features in the prediction of the physical parameters for the experimental setup. Although only six features are used by stepwise regression to model SVI, a different result is possible in the case of other plants operating in different states. The role of the individual classes and their groups is further explored in the perspective of the regression modeling of both SVI and MLSS in the following subsection.

3.3. IDENTIFICATION OF THE CLASSES OF FLOCS FOR THE ESTIMATION

The classification of flocs and their features, concerning equivalent diameter, were tested for their significance in the estimation of SVI and MLSS. The importance of the floc classification was explored in two perspectives: the individual significance of each class and the combined significance of multiple classes together. In other words, it was required to identify individual classes or a combination of the classes, which could lead to the best prediction of SVI and MLSS. To assess the significance in the estimation, the models obtained from the same method of stepwise regression are compared concerning individual and multiple classes. The comparison is carried out using adjusted R^2, and p-value.

When the floc classes were tested individually using stepwise regression, C_2 and C_5 gave higher adjusted R^2 and low p-values. The results are tabulated in Table 7. However, no model could be found with a p-value lower than 0.002, to predict SVI using C_6. This is why C_6 is not present in Table 7. On the other hand, other classes give a p-value less than 0.002 but adjusted R^2 for C_2 and C_5 is better than others.

Next, it was explored if doublets (combining image analysis features corresponding to two floc classes) could improve the model of an individual class as depicted in rows 8–18 in Table 7. When C_2 and C_3 were considered together, adjusted R^2 and p-value of C_2 were not improved by C_3. However, when C_1 was considered with C_2, the adjusted R^2 improved from 0.474 to 0.684. Similar combinations were investigated for C_4, C_5, and C_6. Combining C_6 or C_4 did not result in any improvement in the regression result. However, $C_2 + C_5$, and $C_3 + C_4$ together improved the regression to 0.928 and 0.805, respectively, where + implies inclusion in regression.

After combining two classes, triplets (a group of image analysis features corresponding to three floc classes) were explored to find out if combining individual classes to the doublets improved the results. The adjusted R^2 increased apparently when C_1 was considered together with $C_2 + C_3$. However, this apparent improvement was attributed to the

doublet $C_1 + C_2$. Similarly, triplets formed by combining C_4, C_5 and C_6 to the doublets did not improve the results. However, when a triplet is formed by combining the doublet $C_2 + C_5$ with C_3, the adjusted R^2 improved from 0.928 to 0.951. The best triplet was found to be $C_2 + C_3 + C_5$. It is noteworthy that $C_2 + C_3$ and $C_5 + C_3$ did not improve the regression models of individual classes C_2 and C_5, in doublets, but C_3 did improve the result of the doublet $C_2 + C_5$ to form the best triplet. Subsequently, individual classes and groups of classes were considered together with the best triplet to find out whether the model may be further improved. However, no further improvement was observed. N_A did not show any effect on the estimation of SVI as reflected by row 21, 23, and 30 of Table 7.

T a b l e 7

Floc classification and the predictability of SVI

No.	Floc class	Adjusted R^2	p-Value
1	C_0	0.366	6.28×10^{-4}
2	C_1	0.305	2.04×10^{-3}
3	C_2	0.474	6.09×10^{-5}
4	C_3	0.321	0.00151
5	C_4	0.3	0.00221
6	C_5	0.667	1.25×10^{-6}
8	$C_2 + C_3$	0.474	6.09×10^{-5}
9	$C_1 + C_2$	0.684	2.56×10^{-6}
10	$C_5 + C_2$	0.928	5.52×10^{-11}
11	$C_5 + C_3$	0.667	1.25×10^{-6}
12	$C_1 + C_3$	0.321	0.00151
13	$C_4 + C_5$	0.667	1.25×10^{-6}
14	$C_4 + C_0$	0.596	3.65×10^{-5}
15	$C_4 + C_1$	0.746	2.35×10^{-7}
16	$C_4 + C_3$	0.805	1.32×10^{-8}
17	$C_5 + C_6$	0.667	1.25×10^{-6}
18	$C_4 + C_6$	0.3	0.00221
19	$C_1 + C_2 + C_3$	0.684	2.56×10^{-6}
20	$C_0 + C_4 + C_3$	0.596	3.65×10^{-5}
21	$C_1 + C_2 + C_3 + N_A$	0.684	2.56×10^{-6}
22	$C_4 + C_5 + C_6$	0.667	1.25×10^{-6}
23	$C_4 + C_5 + C_6 + N_A$	0.667	1.25×10^{-6}
24	$C_1 + C_2 + C_5$	0.928	5.52×10^{-11}
25	$C_2 + C_3 + C_5$	0.951	9.21×10^{-12}
26	$C_1 + C_2 + C_4 + C_5$	0.928	5.52×10^{-11}
27	$C_0 + C_1 + C_2 + C_5$	0.928	5.52×10^{-11}
28	$C_1 + C_2 + C_3 + C_5$	0.951	9.21×10^{-12}
29	$C_0 + C_1 + C_2 + C_3 + C_4 + C_5 + C_6$	0.951	9.21×10^{-12}
30	$C_0 + C_1 + C_2 + C_3 + C_4 + C_5 + C_6 + N_A$	0.951	9.21×10^{-12}

Finally, the doublets and triplets were identified with adjusted R^2 greater than 0.8 (the least number of classes and higher adjusted R^2) which were as follows: $C_5 + C_2$, $C_4 + C_3$, and $C_2 + C_3 + C_4$. Hence, C_2, C_3, C_4, and C_5 would be the most significant to predict SVI for an activated sludge plant.

Table 8

Floc classification and predictability of MLSS

No.	Floc class	Adjusted R^2	p-Value
1	C_0	0.394	3.54×10^{-4}
2	C_1	0.268	3.96×10^{-3}
3	C_2	0.364	6.59×10^{-4}
4	C_3	0.291	2.62×10^{-3}
5	C_4	0.334	1.19×10^{-3}
6	C_5	0.495	1.5×10^{-4}
7	N_A	0.685	1.09×10^{-7}
8	$C_2 + C_3$	0.364	0.000659
9	$C_1 + C_2$	0.364	0.000659
10	$C_2 + C_5$	0.548	4.15×10^{-5}
11	$C_3 + C_5$	0.495	0.00015
12	$C_0 + C_5$	0.565	2.68×10^{-5}
13	$C_1 + C_3$	0.291	2.62×10^{-3}
14	$C_4 + C_5$	0.495	1.5×10^{-4}
15	$C_5 + C_6$	0.495	1.5×10^{-4}
16	$C_4 + C_6$	0.492	1.58×10^{-4}
17	$C_0 + C_6$	0.534	5.95×10^{-5}
18	$C_0 + N_A$	0.848	8.62×10^{-10}
19	$C_4 + N_A$	0.808	2.13×10^{-9}
20	$C_5 + N_A$	0.772	1.58×10^{-8}
21	$C_2 + N_A$	0.868	3.04×10^{-11}
22	$C_2 + C_5 + N_A$	0.868	3.04×10^{-11}
23	$C_4 + C_5 + N_A$	0.859	3.81×10^{-10}
24	$C_0 + C_5 + N_A$	0.884	2.42×10^{-10}
25	$C_1 + C_2 + C_3$	0.364	6.59×10^{-4}
26	$C_1 + C_2 + C_3 + N_A$	0.868	3.04×10^{-11}
27	$C_4 + C_5 + C_6$	0.495	1.5×10^{-4}
28	$C_4 + C_5 + C_6 + N_A$	0.859	3.81×10^{-10}
29	$C_1 + C_2 + C_5$	0.548	4.15×10^{-5}
30	$C_2 + C_3 + C_5$	0.548	4.15×10^{-5}
31	$C_1 + C_2 + C_4 + C5$	0.548	4.15×10^{-5}
32	$C_0 + C_1 + C_2 + C_5$	0.565	2.68×10^{-5}
33	$C_1 + C_2 + C_3 + C_5$	0.548	4.15×10^{-5}
34	$C_0 + C_1 + C_2 + C_3 + C_4 + C_5 + C_6$	0.717	7.75×10^{-7}
35	$C_0 + C_1 + C_2 + C_3 + C_4 + C_5 + C_6 + N_A$	0.868	3.04×10^{-11}

To find the significant classes for estimation of MLSS, regression models were first identified for individual classes of flocs. Of all the classes, the class C_5 and the feature N_A gave the best-adjusted R^2. In the next step, doublets were tried and no improvement could be found except for $C_2 + C_5$, $C_5 + N_A$, $C_2 + N_A$, and $C_0 + N_A$, as shown in Table 8. In the table, the other doublets were not included because there was no improvement in the adjusted R^2.

For triplets, considerable improvement in adjusted R^2 was observed only for $C_0 + C_5 + N_A$ and $C_4 + C_5 + N_A$. There was no improvement in all other combinations compared to the doublets. The combinations with the least number of classes and higher adjusted R^2, greater than 0.85, were considered. There were only three such combinations: $C_2 + N_A$, $C_4 + C_5 + N_A$ and $C_0 + C_5 + N_A$. From the combinations, it was concluded that for any regression model, the classes C_0, C_2, C_4 and C_5, and N_A were significant for the estimation of MLSS. Hence, for SVI, C_2, C_3, C_4, and C_5, and for MLSS, C_0, C_2, C_4, C_5, and N_A were important for estimation.

3.4. GENERALIZATION TO MULTIPLE PLANTS

Additional samples from other plants were included to see if the regression model for one plant can be used for other plants under diverse operating states. The SVI and MLSS were again considered separately. The regression models were explored sequentially using the experimental setup, municipal plant K0 with normal samples only, K0 with normal and bulking samples, and all samples from all plants (referred in Tables 1, 2) with and without the bulk. The results are given in Tables 9, 10. In the tables, the features were included with their respective classes, which were selected by stepwise regression models. The selection of classes for the models validates our conclusions drawn in the previous section regarding the significance of classes for regression.

Table 9

Feature selection concerning regression of SVI

Description	Features and their respective class	Adjusted R^2
Experimental setup	C_2^5, C_2^{13}, C_3^9, C_5^2, C_5^7, C_5^{17}	0.951
K0 (normal samples only)	C_4^2, 134	0.755
K0 (normal and bulking samples)	C_4^2, C_5^8	0.726
All samples from all plants (normal samples only)	C_2^{13}, C_5^{16}	0.72
All samples from all plants excluding bulking states	C_1^6, C_4^9, C_4^{14}, C_4^{16}, 134	0.755
All samples from all plants	–	0.246

For individual samples, if the bulking is included, the resultant adjusted R^2 of stepwise regression deteriorates as shown for K0 in Table 9. If the samples are used from all plants together, stepwise regression fails if bulking samples are included. For all

plants, pin-floc/dispersed growth and normal states remain predictable to some extent but bulking fails the prediction. Hence, the data from different plants may be used for estimation of SVI of any plant only if there is a better predictive model, and plants with bulking are excluded. Another observation was the validity of our study in the previous section. Only those classes were selected by stepwise regression, which was proved significant for the estimation of SVI for all scenarios and plants in Table 9.

Table 10

Feature selection concerning regression of MLSS

Description	Features and their respective class	Adjusted R^2
Experimental setup	C_2^{19}, 134	0.868
K0 (normal samples only)	C_3^9	0.353
K0 (normal and bulking samples)	C_4^{18}, C_5^8, 134	0.675
All samples from all plants (normal samples only)	C_2^5	0.4
All samples from all plants excluding bulking states	C_2^{19}, C_0^9, C_2^{10}, C_6^9, 134	0.834
All samples from all plants	C_3^{14}, C_4^8, C_6^9, 134	0.886

Unlike SVI, the adjusted R^2 is improved for diverse operating states and more plants for the stepwise regression for MLSS as shown in Table 10. It is also observed that all the classes recommended for the estimation of MLSS in the previous section are also selected by stepwise regression with one exception. For the case of all plants, a feature from class C_6 was also selected which is given in the last two rows of Table 10. So, individual class C_6 has to be included in the regression model too if more than one plant is being monitored simultaneously.

4. CONCLUSION

Image analysis based modeling of the sludge volume index (SVI) and mixed liquor suspended solids (MLSS) was proposed to monitor the activated sludge process. Such modeling will help time-efficient and clean estimation of SVI and MLSS. It was suggested that an integrated approach for the segmentation of bright-field microscopic images of activated sludge to avoid failure in the segmentation of thousands of images. The flocs were categorized into six classes based on the ranges of equivalent diameter, resulting in 134 image analysis features including an additional proposed feature of N_A. Stepwise regression was used for modeling of SVI and MLSS. Simple models using six and three image analysis features respectively for an experimental setup achieved adjusted R^2 of 0.951 for estimation of SVI, 0.884 for MLSS. The main advantage of the proposed monitoring strategy is the estimation of the physical parameters using flocs

only, without requiring additional protocol to acquire information of filamentous bacteria. Another advantage of this work is the use of only bright-field microscopy at lower magnification without additional requirements on microscopic image acquisition. In this paper, it has been shown that flocs in a certain range of equivalent diameters are more significant to model the physical parameters of SVI and MLSS. Additionally, these significant ranges of equivalent diameters have been identified. The results exhibited consistency when used for regression concerning the shared data for multiple plants and their different states. An innovative idea of a generalization of modeling to monitor the state of multiple plants operating in different states has been introduced. As future work, precise classification of image analysis features needs to be explored to estimate the physical parameters of multiple activated sludge plants using artificial intelligence and big data techniques.

REFERENCES

[1] JENKINS D., RICHARD M.G., DAIGGER G.T., *Manual on the causes and control of activated sludge bulking, foaming, and other solids separation problems*, CRC Press, 2003.
[2] BITTON G., *Wastewater Microbiology*, Wiley, New Jersey 2005.
[3] KHAN M.B., NISAR H., NG C.A., LO P.K., YAP V.V., *Generalized classification modeling of activated sludge process based on microscopic image analysis*, Environ. Technol., 2018, 39 (1), 24–34.
[4] KHAN M.B., NISAR H., NG C.A., LO P.K., *Estimation of sludge volume index (SVI) using bright field activated sludge images*, IEEE International Instrumentation and Measurement Technology Conference, Taipei, Taiwan, 2016, 407–411.
[5] SIKORA M., SMOLKA B., *Feature analysis of activated sludge based on microscopic images*, Canadian Conference on Electrical and Computer Engineering, Toronto, Ontario, 2001, 2, 1309–1314.
[6] JENNE R., CENENS C., GEERAERD A.H., IMPE J.F., *Towards on-line quantification of flocs and filaments by image analysis*, Biotechnol. Lett., 2002, 931–935.
[7] HEINE W., SEKOULOV I., BURKHARDT H., BERGEN L., BEHRENDT J., *Early warning system for operation failures in biological stages of WWTPs by online image analysis*, Water Sci. Technol., 2002, 46 (4–5), 117–124.
[8] PEREZ Y.G., LEITE S.G.F., COELHO M.A.Z., *Activated sludge morphology characterisation through an image analysis procedure*, Brazilian J. Chem. Eng., 2006, 319–330.
[9] KHAN M.B., NISAR H., NG C.A., LO P.K., *A vignetting correction algorithm for bright-field microscopic images of activated sludge*, International Conference on Digital Image Computing: Techniques and Applications (DICTA), Gpld Coast, QLD, Australia, 2016, 1–4.
[10] FISHER R., PERKINS S., WALKER A., WOLFART E., *Hypermedia Image Processing Reference (HIPR)*, John Wiley & Sons, 1996.
[11] KHAN M.B., NISAR H., NG C.A., LO P.K., YAP V.V., *Local adaptive approach toward segmentation of microscopic images of activated sludge flocs*, J. Electron. Imaging, 2015, 24 (6), 061102-10.
[12] MESQUITA D.P., AMARAL A.L., FERREIRA E.C., *Estimation of effluent quality parameters from an activated sludge system using quantitative image analysis*, Chem. Eng. J., 2016, 285, 349–357.
[13] AMARAL A.L., MESQUITA D.P., FERREIRA E.C., *Automatic identification of activated sludge disturbances and assessment of operational parameters*, Chemosphere, 2013, 91 (5), 705–710.
[14] BOZTOPRAK H., ÖZBAY Y., GÜÇLÜ D., KÜÇÜKHEMEK M., *Prediction of sludge volume index bulking using image analysis and neural network at a full-scale activated sludge plant*, Desalin. Water Treat., 2015, 57 (37), 17195–17205.

[15] TOMPERI J., KOIVURANTA E., KUOKKANEN A., JUUSO E., LEIVISKÄ K., *Real-time optical monitoring of the wastewater treatment process*, Environ. Technol., 2016, 37 (3), 344–351.

[16] TOMPERI J., LEIVISKÄ K., *Comparison of modeling accuracy with and without exploiting automated optical monitoring information in predicting the treated wastewater quality*, Environ. Technol., 2018, 39 (11),1442–1449.

[17] HONGGUI H., YING L., JUNFEI Q., *A fuzzy neural network approach for online fault detection in wastewater treatment process*, Comput. Electr. Eng., 2014, 40 (7), 2216–2226.

[18] TOET S., LOGTESTIJN R.S.P., KAMPF R., SCHREIJER M., VERHOEVEN J.T.A., *The effect of hydraulic retention time on the removal of pollutants from sewage treatment plant effluent in a surface-flow wetland system*, Wetlands, 2005, 25 (2), 375–391.

[19] KHAN M.B., NISAR H., NG C.A., LO P.K., *Illumination compensated segmentation of microscopic images of activated sludge flocs*, International Conference on Digital Image Computing: Techniques and Applications (DICTA), Adelaide, SA, Australia, 2015, 1–5.

[20] RUSS J.C., *The image processing handbook*, CRC Press, Boca Raton, FL, 2011.

[21] OBERT M., *Numerical estimates of the fractal dimension D and the lacunarity L by the mass radius relation*, Fractals, 1993, 1 (3), 711–721.

[22] DRAPER N.R., SMITH H., *Applied Regression Analysis*, John Wiley & Sons, 1998.